Measuring Individual Battery Dimensional Changes for State-of-Charge Estimation using Strain Gauge Sensors

***Abstract*—This paper experimentally studies the mounting of strain gauges on the cases of Lithium-Ion battery cells for the purpose of correlating the battery dimensional changes (e.g., strain measurement) to the real-time State-of-Charge (SOC). The paper first investigates the placement of the strain gauge sensor and the resulting measured strain profile during a constant-current-constant-voltage (CCCV) cycle, demonstrating that it contains useful information that can be correlated with the SOC. The battery dimensional change polarization following a current event is then investigated to determine whether the rest time that is required when using the open-circuit voltage for SOC estimation can be reduced in order to increase the total energy throughput of a battery pack. Key conclusions are that the strain gauges generate output voltages that track the SOC profile during dynamic charge/discharge events, and that strain gauges holds promise for significantly reducing the rest time that is currently required for estimating SOC in many applications.**

I. Introduction

Lithium-Ion battery systems typically require accurate and reliable state-of-charge (SOC) estimation in most applications. Excellent examples are large battery systems found in battery-electric vehicles [1] and Distributed-Energy-Storage (DES) applications [2]. Monitoring and estimation of SOC in real-time is a heavily researched topic in both academia and industry, with numerous methods for calculation. The most common method is Coulomb Counting (or Ah Counting), but over large periods of time this method accumulates some error that needs to be accounted for with additional estimation methods [3]. One method for correcting this model error has been by correlating the open-circuit-voltage (OCV) to the battery SOC. Unfortunately, this correlation requires significant rest time for the battery prior to being able to accurately estimate the battery SOC [4]. Other methods that are more complicated and computationally-intensive have been developed, often using Kalman filtering for SOC estimation. However, errors still tend to accumulate, albeit at slower rates, so the OCV-SOC method continues to be used to improve the SOC estimation [5].

Since the OCV-SOC method is still heavily utilized across numerous SOC estimation methods, techniques to improve the accuracy and time needed for SOC estimation are still being sought. A key issue with the OCV-SOC lookup method is the demand for rest time to accurately predict the SOC. That is, the battery needs to be at rest for 10 minutes or more before performing an SOC adjustment in DES applications according to [6]. Developing new methods to reduce/mitigate this rest time is highly desired by commercial suppliers since this rest time can accumulate to significant total time each year during which the battery is prevented from delivering energy throughput to the load, with economic consequences.

Rest time is needed when using the OCV for SOC estimation due to the polarization of the battery voltage during a charge/discharge event. In order to reduce/mitigate this rest time, alternative techniques for estimating battery SOC are desired. Previous studies have shown that a battery at full SOC results in a thickness change of up to 10.4% due to the graphite anode volumetric increase that is not reciprocated on the cathode material side [7], [8]. Due to this observed dimensional change, some past research has focused on understanding how the dimensional changes of the battery correlates to either the battery voltage or SOC. Studies have shown that the battery dimension changes exhibit a similar profile as the open-circuit voltage, and the similarity between these profiles depends on the cell casing, e.g., pouch cell vs. can [9]. This research showed that the battery thickness tracks the same profile as the voltage, so a thickness-SOC correlation can be made that is similar to the OCV-SOC correlation currently performed. However, a key question left unanswered is how the battery thickness polarizes after a charge/discharge current event. If the thickness polarizes much less than the voltage, then using the battery thickness as basis for SOC estimation will result in a significant reduction in the rest time in practical applications. However, the research in [9] used position sensors to measure the thickness of the tested battery at all times. While this can be an accurate method, the use of position sensors would not be practical in applications where the battery pack contains large number of batteries due to the sensor cost and mass/volume.

In order to find a more compact and economical battery dimensional change measurement method, research has been conducted to investigate the use of a strain gauge to correlate the strain changes to the battery thickness changes, and, ultimately, to the SOC changes [10]. However, it is important to note that this prior work measured the lumped strain of 5 Lithium-Ion batteries, since the strain gauge was mounted on the tie-rod holding the 5 batteries together.

The purpose of this paper is to investigate whether useful strain-SOC correlation can be derived from strain gauges that are directly mounted on individual battery cells, so that every cell can have its own strain-SOC lookup to track the performance of individual batteries. This investigation has studied whether placing a strain gauge on each individual battery contains sufficient strain-change to be able to exhibit a useful strain-voltage profile correlation. Importantly, this investigation also studies the polarization of battery dimensional changes (e.g., strain or thickness measurement) after a current event to evaluate the potential of this technique to mitigate/reduce the rest time needed for SOC adjustments.

II. Experimental Setup

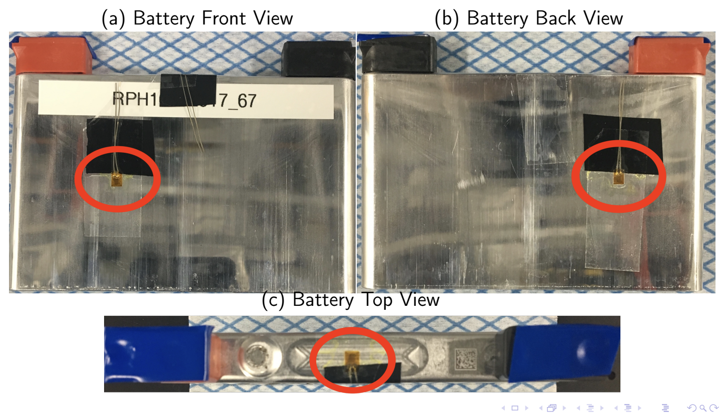

Fig. 1 Location of strain gauge placement on the battery, where (a) shows the position of "Strain Gauge #1" on the front surface of the battery, (b) shows the position of "Strain Gauge #2" on the back surface of the battery, and (c) shows the position of "Strain Gauge #3" on the top surface of the battery (over the vent region). The thickness gauge probe points (not shown) were positioned at the direct centers of the front and back surfaces in (a) and (b).

The experiments in this paper were performed by synchronizing multiple measurement systems in order to accurately and reliably measure battery electrical, strain, and thickness parameters for the desired battery test profiles. The batteries were tested using Digatron cycling equipment which made it convenient to apply precise and accurate charge/ discharge profiles that were pre-determined for each experiment. The strain gauge outputs were measured using a half-bridge version of the Wheatstone bridge combined with noise reduction techniques found in [11] to reduce measurement errors. The output voltage of the Wheatstone bridge was measured using the Digatron system, and the accumulated data was post-processed to convert the bridge output voltages to strain. The thickness sensor was a Mitutoyo position sensor that utilized a Versatile Data Acquisition System (VDAS) to monitor the battery thickness. The VDAS system also recorded the battery voltage in order to synchronize the Digatron test data with the VDAS test data.

The batteries used in this paper were 5.5Ah rated batteries from Johnson Controls, and the experiments utilized multiple cells for each experiment, with representative data for each experiment being shown [6]. Perhaps the most critical aspect of this study was to understand the significance of the strain gauge placement location and the resulting strain similarity to the voltage profile. Fig. 1 shows the strain gauge locations on the battery for all of the experiments in this paper, where (a) shows the position of "Strain Gauge #1" on one battery surface, (b) shows the position of "Strain Gauge #2" on the other battery surface, and (c) shows the position of "Strain Gauge #3" on the top surface at the center of the thinned vent region. Strain Gauges #1 and #2 are intentionally offset from center of the two battery surfaces so that the thickness sensor probe can be placed directly in the center. His prevents the position probe from touching, or affected the strain gauges.

Strain Gauge #3 was placed over the overpressure vent. The vent location is a region of the battery case that has a thinner metal casing material by design, which intentionally ruptures if the internal pressure of the battery becomes dangerously high. This rupturing is a last-resort means to vent the cell to the ambient environment to prevent more dangerous events such as thermal runaway. The reason for placing a strain gauge on this location was to determine if the thinner metal casing would exhibit more deflection (i.e., strain) during the charge/discharge events. Since previous research had not mounted strain gauges directly onto battery surfaces, engineering judgment was used to identify the surface locations with the highest potential for providing strain measurements that would be for useful for estimating the SOC.

III. Experimental Evaluation for Measurement of Battery Dimensional Changes

While the ultimate goal of this project was to understand if battery dimensional changes could be used as an SOC estimation technique, the first step was to determine how well the installed strain gauges and position sensor could track the dimensional changes of an individual battery rather than a group of several batteries. This was accompanied by tests to determine how well these sensors can track the battery terminal voltage, and ultimately the battery SOC, during dynamic charging and discharge events.

A. Strain Gauge Mounted on Battery Cell for Dimensional Changes Measurement

The first experiment that was performed was a single constant-current/constant-voltage (CCCV) cycle in order to directly compare the profile for the battery voltage, and the various dimensional change sensors. Fig. 2 shows four experimental plots, each comparing the battery terminal voltage profile during a single discharge/charge event with the sensor voltage plot for one of the four dimensional change sensors, as follows: (a) Strain Gauge #1 on the front surface, (b) Strain Gauge #2 on the back surface, (c) Strain Gauge #3 on the top surface vent, and (d) the thickness sensor spanning the front and back surfaces. The blue voltage trace is linked to the primary (left-side) *y*-axis scale, and the red trace for the dimensional change sensor is linked to the secondary (right-side) *y*-axis scale.

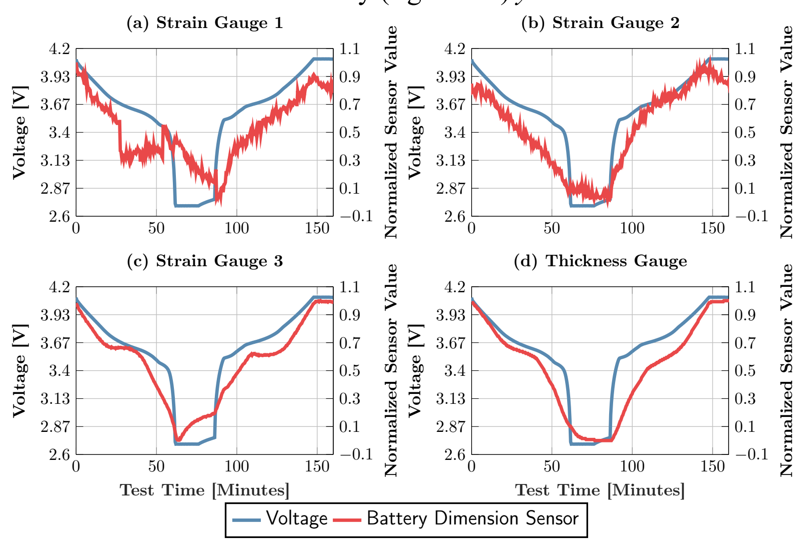

Fig. 2 Single-cycle CCCV experimental results comparing the measured battery voltage plot to the sensor measurement from one of the four dimensional change sensors: (a) Strain gauge #1, (b) Strain gauge #2, (c) Strain gauge #3, and (d) Thickness gauge

Analyzing the experimental results in Fig. 2 leads to two key conclusions. First, all of the four dimensional change sensors deliver output voltages that exhibit varying levels of correlation with the battery voltage waveform. In particular, Strain Gauges #2 and #3 and the thickness gauge deliver voltage waveforms with promising similarity to the battery voltage waveform for the CCCV cycle. These results suggest that battery dimensional changes measured locally on a battery offer promise for SOC estimation, avoiding the need to monitor the aggregate strain of a string of batteries.

Secondly, this experiment has highlighted the significance of the strain gauge location on the amplitude and quality of the sensor output waveforms. Although the output voltages for all of the dimensional change sensors in Fig. 2 are plotted on normalized scales, examination of the underlying data reveals that the peak-to-peak amplitude of the output voltage for Strain Gauge #3 on the thinned vent is approx. 10 times the corresponding peak-to-peak voltage amplitudes for Strain Gauges #1 and #2 on the front and back battery surfaces. As a result, the output voltage for Strain Gauge #3 exhibits far less noise than the corresponding waveforms for Strain Gauges #1 and #2, strengthening the case that the thinned vent is, as hypothesized, a preferred location for measuring the dimensional change during battery operation. Another way to interpret these results is that there are opportunities to optimize both the amplitude and the quality of strain gauge sensor signals by specially designing the battery case in the regions where the strain gauges are mounted.

B. Battery Dimensional Sensor Behavior during Extended Cycling Test

Next, the measured characteristics of the strain gauge output voltage waveforms during the course of several sequential battery cycles was investigated to explore the stability of the correlation between these sensor voltages and the battery terminal voltage. Based on the desirable performance features of Strain Gauge #3 compared to those of Strain Gauges #1 and #2 in the preceding tests, only the experimental results for

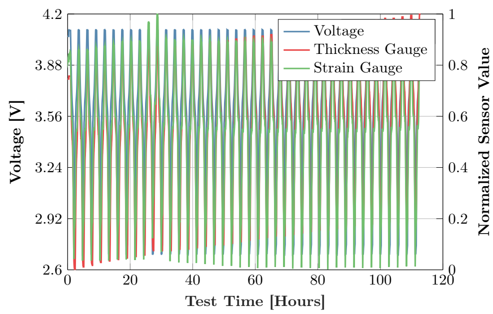

Fig. 3 Multiple cycles analysis of thickness and strain sensor relationships to battery voltage.

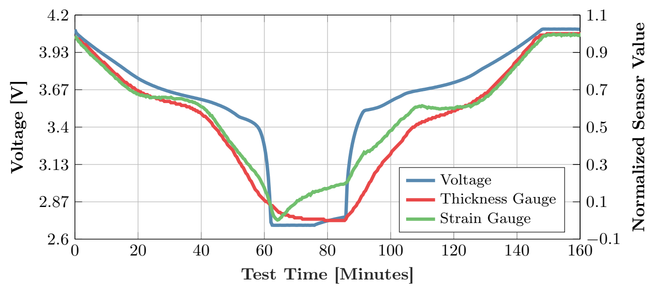

Fig. 4 Single cycle view of voltage, strain, and thickness sensor relationship extracted from the cycling analysis.

Strain Gauge #3 (henceforth denoted as simply the strain gauge) will be presented for comparison with the output voltage of the thickness gauge and the battery terminal voltage. This repetitive cycling experiment again used discharge/charge CCCV cycles, repeated 40 times to investigate how the correlation between the dimensional change sensor voltages and the battery voltage evolves over many cycles. Fig. 3 shows the overlaid waveforms for the battery voltage and the two types of battery dimensional change sensors (thickness and strain gauges) during 40 repeated CCCV discharge/charge cycles.

Examining the waveform results during the cycling test in Fig. 3, the profiles of all three sensors (voltage on the primary *y*-axis, and strain/thickness sensor on right-side secondary *y*-axis) exhibit similarity during all of the cycles. This correlation is consistently evident in all of the cycles throughout the 110 hours of testing. Fig. 4 provides an expanded view of a single cycle during the cycling test in Fig. 3, highlighting the promising level of correlation between the output signals from the three sensor types.

While both normalized peak-to-peak amplitudes of all three sensors are relatively constant throughout the 40 cycles, some features of the envelopes for the two dimensional sensors in Fig. 3 deserve comment. The thickness gauge envelope voltages gradually increase during the test, a feature that can be attributed to the solid electrolyte interphase (SEI) layer growth and progressive battery case expansion during aging as discussed in [9]. Shifting attention to the strain gauge, its envelope voltage in Fig. 3 increased unexpectedly during 2 cycles approx. 30 hours after the test begun. Closer investigation revealed that external vibrations caused by other dynamometer equipment in the same room were the source of the disturbance in the strain gauge test results. Finding ways to suppress this sensitivity to external vibrations applied to the test battery assembly represents an engineering challenge that will require a solution if there is an interest in applying this strain gauge technique in environments such as automobiles where such vibrations are expected.

C. Polarization Investigation of Battery Dimensional Changes following Discharge Current Event

Based on the experimental results gathered during this study, the strain gauge sensor has demonstrated significant promise as a means of monitoring the battery's dimensional changes, but the vulnerability of the battery dimensional changes to polarization still requires discussion. To explore this issue, an experiment was conducted consisting of a 0.5 C-rate discharge until 0.5Ah was removed from the battery (initially at 100% SOC), after which the battery was allowed to rest for 1 hour to monitor any evidence of polarization. The 0.5Ah discharge cutoff was designed to interrupt the current and proceed immediately to a rest condition before the battery was fully discharged. As a result, the battery voltage was still decreasing up to the moment of cutoff, creating favorable conditions for examining the polarization issue. Fig. 4 Single cycle view of voltage, strain, and thickness sensor relationship extracted from the cycling analysis. shows the results from this experiment, with the battery voltage mapped to the primary *y*-axis, and the output of the normalized strain and thickness sensors mapped to the secondary *y*-axis.

The measured results from this experiment in Fig. 5 show that the discharge current was interrupted at approx. 23 minutes after the test began, and the system transitioned to its rest state during the next several minutes. In particular, the measured terminal voltage significantly polarizes (i.e., increases) from approx. 3.79V to 3.82V during the next 45 minutes. Since typical applications perform the OCV-SOC lookup after a rest period of approx. 5 to 10 minutes, the results of this experiment indicate that the battery terminal

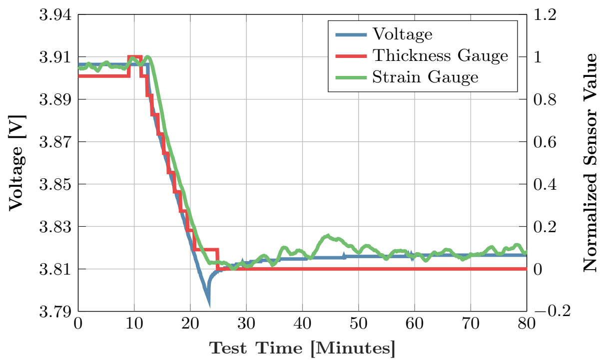

Fig. 5 Discharge pulse (0.5 C-Rate) followed by 1 hour rest period to understand polarization of battery dimensional change relative to voltage polarization.

voltage has not yet reached its steady-state value during this shortened time interval, raising the risk of errors attributable to use of the open-circuit voltage for estimating the SOC. In contrast, the battery thickness sensor reaches its steady-state within 1 minute of the rest state initiation. While the strain gauge output voltage does not settle to a constant voltage during the rest period, it also appears to exhibit much lower polarization effects than the open-circuit voltage. The variations that appear in the strain gauge voltage during the rest period can be significantly reduced by improving the strain gauge implementation beyond the simplified version adopted for this proof-of-concept experiment, a target for future work.

IV. Conclusions

The results of this paper provide clear evidence that dimensional changes of a single battery cell measured using either a thickness sensor or strain gauges provides useful information about the battery's state-of-charge that is much freer from polarization effects than the open-circuit voltage that is commonly used to estimate the battery's SOC today. In particular, the strain gauge was shown to be an appealing candidate for measuring the dimensional changes because it is much less obtrusive and lower in cost than a thickness sensor. This investigation has demonstrated that the location chosen for mounting the strain gauge on the battery case is critical to the overall success of the sensor measurement. The test results support the conclusion that designing a special surface area on the battery case to mount the strain gauge can significantly enhance the sensor measurements.

Test results showed that the strain gauges and thickness sensor both exhibit waveform profiles during CCCV cycling that are similar to those of the open-circuit voltage, suggesting that the strain gauges hold promise for estimating the battery SOC as a practical alternative to the OCV. Further testing showed that the battery terminal voltage exhibits the expected polarization effects that, in practice, require rest times to eliminate SOC estimation errors. In contrast, the thickness sensor and strain gauge exhibited much lower polarization effects that hold promise for significantly reducing or even eliminating the rest time needed for SOC estimation.

Limitations of the simplified strain gauge implementation used during these initial tests highlighted the need for further work to improve the quality of their output signals and to reduce their sensitivity to external vibration sources. Nevertheless, the completed tests confirmed that strain gauges offer some intriguing features as a potential alternative to the baseline open-circuit voltage technique for estimating battery cell SOC that merit further investigation.

References

[1] Y. Xing *et al.*, "Battery Management Systems in Electric and Hybrid Vehicles," *Energies*, 4(11), pp. 1840–57, Oct. 2011.

[2] G. (Gianfranco) Pistoia, *Lithium-ion batteries : advances and applications*.

[3] K. S. Ng, C. S. Moo, Y. P. Chen, and Y. C. Hsieh, "Enhanced coulomb counting method for estimating state-of-charge and state-of-health of lithium-ion batteries," *Appl. Energy*, vol. 86, no. 9, pp. 1506–1511, 2009.

[4] S. J. Lee, J. H. Kim, J. M. Lee, and B. H. Cho, "The State and Parameter Estimation of an Li-Ion Battery Using a New OCV-SOC Concept," *2007 IEEE Power Electron. Spec. Conf.*, no. July, pp. 2799–2803, 2007.

[5] F. Sun, X. Hu, Y. Zou, and S. Li, "Adaptive unscented Kalman filtering for state of charge estimation of a lithium-ion battery for electric vehicles," *Energy*, vol. 36, pp. 3531–3540, 2011.

[6] JCI, "Johnson Controls - Power Solutions," 2016. [Online]. Available: https://www.johnsoncontrols.com/suppliers/batteries.

[7] S. Konar, U. Hä, and G. Svensson, "Intercalation Compounds from LiH and Graphite: Relative Stability of Metastable Stages and Thermodynamic Stability of Dilute Stage I d," 2015.

[8] Y. Qi and S. J. Harris, "In Situ Observation of Strains during Lithiation of a Graphite Electrode," 2010.

[9] J. H. Lee, H. M. Lee, and S. Ahn, "Battery dimensional changes occurring during charge/discharge cycles - Thin rectangular lithium ion and polymer cells," *J. Power Sources*, vol. 119–121, pp. 833–837, 2003.

[10] X. Wang, Y. Sone, G. Segami, H. Naito, C. Yamada, and K. Kibe, "Understanding Volume Change in Lithium-Ion Cells

during Charging and Discharging Using In Situ Measurements," *J. Electrochem. Soc.*, vol. 154, no. 1, p. A14, 2007.
[11] S. Gages, "Errors Due to Shared Leadwires in Parallel Strain Gage Circuits TN-516," pp. 163–168, 2010.